RAPID COMMUNICATION

One ε-Ga_2O_3-based solar-blind Schottky photodetector emphasizing high photocurrent gain and photocurrent-intensity linearity

Yue-Hua An(安跃华)[1], Zhen-Sen Gao(高震森)[2,†], Yu Guo(郭雨)[1], Shao-Hui Zhang(张少辉)[4], Zeng Liu(刘增)[3,‡], and Wei-Hua Tang(唐为华)[3,§]

[1] *School of Optoelectronic Engineering, Guangdong Polytechnic Normal University, Guangzhou* 510665, *China*
[2] *School of Information Engineering, Guangdong University of Technology, Guangzhou* 510006, *China*
[3] *Innovation Center for Gallium Oxide Semiconductor (IC-GAO), College of Integrated Circuit Science and Engineering, Nanjing University of Posts and Telecommunications, Nanjing* 210023, *China*
[4] *Institute of Microscale Optoelectronics, College of Physics and Optoelectronic Engineering, Shenzhen University, Shenzhen* 518060, *China*

(Received 11 September 2022; revised manuscript received 13 January 2023; accepted manuscript online 31 January 2023)

The ε-Ga_2O_3 thin film was grown on sapphire substrate by using metalorganic chemical vapor deposition (MOCVD) method, and then was used to fabricate a deep-ultraviolet (DUV) photodetector (PD). The ε-Ga_2O_3 thin film shown good crystal quality and decent surface morphology. Irradiated by a 254-nm DUV light, the photodetector displayed good optoelectronic performance and high wavelength selectivity, such as photoresponsivity (R) of 175.69 A/W, detectivity (D^*) of 2.46×10^{15} Jones, external quantum efficiency (EQE) of 8.6×10^4% and good photocurrent-intensity linearity, suggesting decent DUV photosensing performance. At 5 V and under illumination with light intensity of 800 μW/cm^2, the photocurrent gain is as high as 859 owing to the recycling gain mechanism and delayed carrier recombination; and the photocurrent gain decreases as the incident light intensity increases because of the recombination of photogenerated carriers by the large photon flux.

Keywords: metastable Ga_2O_3, photocurrent gain, linearity, DUV detection

PACS: 85.60.Gz, 42.60.Lh **DOI:** 10.1088/1674-1056/acb75b

1. Introduction

In order to be answerable for the gradually ascending demands of performance and speed in the modern electronics and optoelectronics in the near future, wide band-gap (E_g) semiconductors, such as gallium nitride (GaN), silicon carbide (SiC), gallium oxide (Ga_2O_3), diamond, and aluminum nitride (AlN), *etc.*, are put forward and have gained lots of research enthusiasm[1,2] for the whole or part supplements in mature silicon-based ICs. Although encountering the difficulties of p-doping and device processing, Ga_2O_3 unfold its superiority before researchers' eyes around the world in terms of solar-blind deep ultraviolet (DUV) photodetectors and high-power devices, owing to its appropriate properties in nature.[3–5] The E_g of ~ 4.9 eV allows Ga_2O_3 to have strong absorbance in the DUV region, thus Ga_2O_3 is quite suitable for constructing DUV photodetectors.[3,6]

Currently, a great deal of researches has been focused on the photodetectors based on semiconducting Ga_2O_3 materials. For instance, Qian *et al.*[7] reported a super-sensitive β-Ga_2O_3-based photodetector with specific detectivity (D^*) of 4.22×10^{15} Jones by a high-density Al@Al_2O_3 core–shell nanoplasmonic array. Zhi *et al.*[8] used metalorganic chemical vapor deposition (MOCVD)-grown β-Ga_2O_3 thin film to fabricate a linear solar-blind photodetector array, showing high photoresponse and decent standard deviation of photo responsivity (R). Benefiting from the tunable currents in channel by gate voltage, the Ga_2O_3-based phototransistors were also displayed of high R, D^*, and good photocurrent (I_{photo}) linearity.[9–11] For the Schottky photodiode structure, Liu *et al.*[12] shown a high-performance device of high R and good wavelength selectivity; and the enhanced performances were discussed in the metal–oxide–semiconductor (MOS)[13] and trench[14] photodiodes. In spite of these, Schottky photodiode (and some photovoltaic detectors) should not have gain (G) essentially, unless that it is breakdown. In general, the high photoresponse and fast response speed is always a hard issue to compromise;[15–19] Zhou *et al.*[17] portrayed a Ga_2O_3 broadband photodetector with a high G of 5438, while its recover time is as long as 9 s due to the persistent photoconductivity (PPC) effect.[18] At present, β-Ga_2O_3 is the most common investegated subject, while, the metastable Ga_2O_3 also displays some advantages and is worthy researching.[20,21] In the photodetecting devices, the surface trapping caused by the existence of surface states and defects are always influencing the photo sensing performances of a photodetector,[22–25] to a large extent. However, ε-Ga_2O_3 is less reported in

†Corresponding author. E-mail: gaozhensen@gdut.edu.cn
‡Corresponding author. E-mail: zengliu@njupt.edu.cn
§Corresponding author. E-mail: whtang@njupt.edu.cn

© 2023 Chinese Physical Society and IOP Publishing Ltd

this field. In comparison to extensively studied stable β-Ga_2O_3, metastable ε-Ga_2O_3 has a hexagonal structure like some other wide bandgap semiconductors,[21] such as GaN, SiC, and ZnO, *etc.*[26,27] With them, ε-Ga_2O_3 could be constructed in heterojunction structures with relatively low lattice mismatches. However, there are only a limited number of reports on ε-Ga_2O_3 photodetectors, the research on the ε-Ga_2O_3 photodetectors remained unclear, especially for the gain mechanism.

Therefore, in this work, the metastable ε-Ga_2O_3 thin film was prepared by utilizing MOCVD technique, then was patterned with interdigital Ni/Au bilayer electrode with five fingers for finishing the photodetector in construction. The x-ray diffraction (XRD) and atomic force microscope (AFM) were employed to characterize the crystal quality of prepared β-Ga_2O_3 thin film. Through a Keithley 4200 semiconductor analyzer, the current–voltage (I–V) and transient photo-response (*i.e.*, I–t performance) were measured. Together with R and external quantum efficiency (EQE), the G and response time are discussed in detail, in the view of surface trapping in metal-Ga_2O_3 Schottky photodetector.

2. Experimental details

The ε-Ga_2O_3 thin film was grown by using MOCVD equipment at substrate temperature of 750 °C and chamber pressure of 25 Torr (1 Torr = 1.33322×10^2 Pa), with the triethylgallium (TEGa) and 99.999% pure O_2 as Ga and O precursors.[28] The TEGa was stored in a stainless-steel bubbler of 35 °C temperature and 760-Torr pressure. Especially, the oxygen-to-gallium [O/Ga] ratio is about 1600 according to Antoine's equation,[29] upon an oxygen gas flow ratio of $\sim$ 6000 SCCM.

The quality of the prepared film was verified by employing XRD and AFM for its degree of crystallinity, surface morphology, and roughness. And, the optical E_g was obtained via measuring the absorbance spectrum of the ε-Ga_2O_3 thin film. Always, due to the distinct surface charge accumulation layer in oxide semiconductor (including the Ga_2O_3 discussed in this work), the O_2 plasmas was used to surface-treat the ε-Ga_2O_3 thin film for 30 seconds before device construction[30,31] so as to achieve decent Schottky contact. Then, with ion beam sputtering methods to use, a five-pairs interdigital Ni/Au bilayer electrode was patterned on the surface of the ε-Ga_2O_3 thin film along with 190-μm length, 5-μm width, and 5 μm in spacing gap, translating to an effective irradiated area of 9.5×10^3 μm^2 as calculated by the device scales. In this procedure, according to the Schottky–Mott rule, the Ni was chosen to act as the Schottky metal, as the work function of Ni (Φ(Ni)) is higher than the electron affinity of Ga_2O_3 ($\psi(Ga_2O_3)$).

In term of characterization of photodetector, on behalf of characterizing the DUV optoelectronic performances of the photodetector, the typical I–V and I–t behaviors were measured by virtue of a semiconductor analyzer called Keithley 4200 in the air at room temperature (about 24 °C). During which, a lamp that could emit 254-nm UV light was used as the irradiated source with tunable light intensity via changing the distance between samples and the light source; the light intensity could be read out by a display instrument.

3. Results and discussion

In Fig. 1(a), the XRD pattern of the MOCVD-grown Ga_2O_3 thin film is displayed, suggesting the (002), (004), and (006) crystal planes, the results verified the ε-Ga_2O_3 existence; in which the sharp (0006) diffraction peak is from the sapphire substrate for Ga_2O_3 thin film deposition. Figure 1(b) is the two-dimensiond (2D) AFM image of the surface of ε-Ga_2O_3 thin film, verifying uniform claviform grains and good crystallization. In Fig. 1(c), it shows the three-dimensional (3D) AFM image of the surface of ε-Ga_2O_3 thin film, from which the root-mean-square (RMS) roughness of 13.1 nm for the MOCVD-grown ε-Ga_2O_3 thin film can be obtained. To a large extent, the quality of the film crystal is necessary for determining the electronic device performance. On the basis of this prepared ε-Ga_2O_3 thin film, the schematic diagram of the ε-Ga_2O_3 DUV photodetector is shown in Fig. 1(d), as described in the experimental section. It is a typical metal–semiconductor–metal (MSM) photodetector device with five fingers. As seen from Fig. 2, the absorbance spectrum of the ε-Ga_2O_3 thin film is displayed, indicating the stronger absorbance in the DUV region than that in visible region; and the optical E_g of $\sim$ 5.01 eV is obtained via Tauc relationship: $(\alpha hv)^2$ *versus* hv (photon energy) as shown in the inset of Fig. 2. In addition, the response spectrum of the ε-Ga_2O_3 photodetector is displayed in Fig. 3, showing the

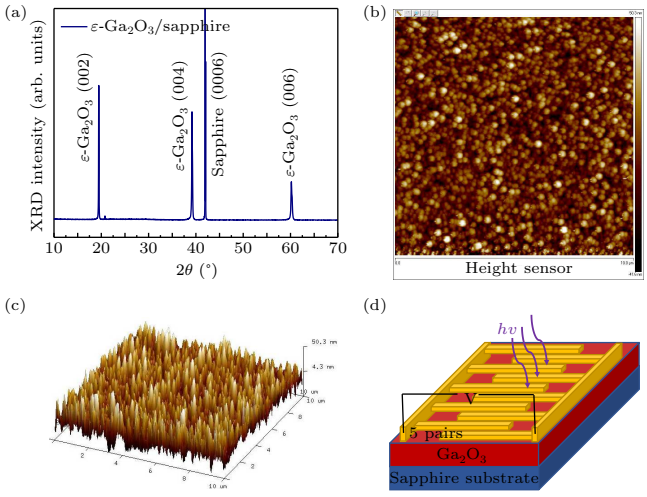


Fig. 1. (a) The XRD pattern, (b) 2D and (c) 3D AFM images of the surface of ε-Ga_2O_3 thin film of the MOCVD-grown ε-Ga_2O_3 thin film on sapphire substrate. Based on which, panel (d) is the schematic diagram of the photodetector.

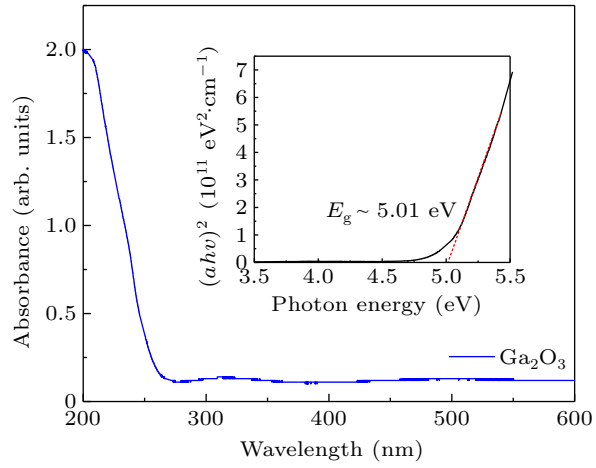


Fig. 2. The absorbance spectrum of the MOCVD-grown ε-Ga_2O_3 thin film.

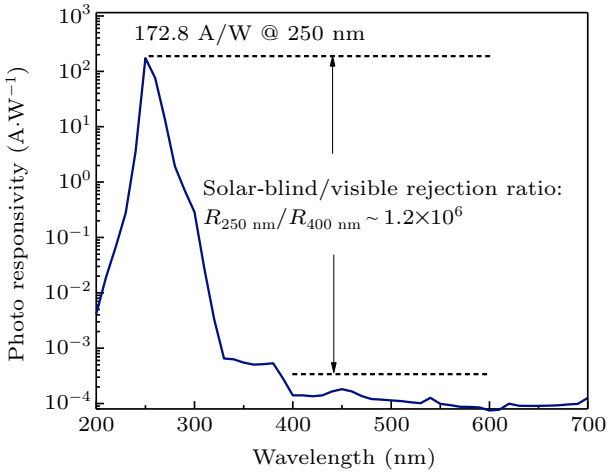


Fig. 3. The response spectrum of the ε-Ga_2O_3 photodetector.

strongest photo response in the solar-blind UV region, compared to the other wavebands. The solar-blind/visible rejection ratio ($R_{250\ nm}/R_{400\ nm}$) is up to 1.2×10^6, suggesting excellent wavelength selectivity. And, the peak responsivity (R) is about 172.8 A/W at 250-nm light irradiation.

As shown in Fig. 4(a), the linear I–V curve of the ε-Ga_2O_3 thin film photodetector is shown in the dark and under DUV light illumination. In the dark case, as displayed in the inset of Fig. 4(a), the photodetector shows Schottky electronic behavior due to the difference between the work function of metal electrode (Ni ~ 5.15 eV) and the electron affinity of Ga_2O_3 (~ 4.00 eV), according to the Schottky–Mott rule.[28] In which, the I–V behavior can be described by thermionic emission rule as follows:

$$I = I_0\left[\exp\left(\frac{qV}{nkT}\right)-1\right], \tag{1}$$

$$I_0 = AA^*T^2\exp\left(-\frac{\varphi_B}{kT}\right), \tag{2}$$

where I_0 is the saturation current, A is the area of metal–semiconductor contact, k is the Boltzmann constant, φ_B is the Schottky barrier height

$$\varphi_B = \frac{kT}{q}\ln\left(\frac{AA^*T^2}{I_0}\right),$$

A^* is the efficient Richardson constant and is always shown as

$$A^* = \frac{4\pi qm^*k^2}{h^3}, \tag{3}$$

where h is the Planck constant, m^* is $0.342m$ for Ga_2O_3, m is the free electron mass. At 5-V bias, the dark current (I_{dark}) is ~ 1.52 pA, suggesting low noise performance when considering I_{dark} as the main noise in this ε-Ga_2O_3 thin film photodetector,[32] owing to the carrier constraint by interfacial Schottky barrier. According to Eqs. (1)–(3), the φ_B is determined to be 0.56 eV under the dark condition.[33] This kind photodetector with a barrier to constrain carrier transports could generate more desired photodetection performance, compared to Ohmic-type photodetector.[28] At 5 V, under illumination with light intensity of 800 μW/cm^2, the photo-to-dark current ratio (PDCR) is as high as 8.78×10^6 as shown in Fig. 4(b), it verifies the high DUV photoresponse; in other word, the output current increases six orders of magnitudes when it is illuminated by 254-nm DUV light. In order to characterize the DUV photoresponse in detail, photoresponsivity (R), detectivity (D^*), and external quantum efficiency (EQE) are introduced for specific characterization. They can be shown as[34]

$$R = \frac{I_{photo}-I_{dark}}{PS}, \tag{4}$$

$$D = \frac{R}{\sqrt{2qI_{dark}/S}}, \tag{5}$$

$$\mathrm{EQE} = \frac{hvR}{e}, \tag{6}$$

where I_{photo} is the photocurrent, P is the light intensity, S is the efficient illuminated area of the photodetector, e is the electron charge, v is the frequency of incident light. At 5 V, under illumination with light intensity of 800 μW/cm^2, the R is calculated to be 175.69 A/W, and D^* is 2.46×10^{15} cm·Hz$^{1/2}$·W^{-1} (Jones) based on Eqs. (4) and (5), those certify the high DUV photoresponse property and low signal/noise performance. For calculating the D^*, the I_{dark} (external noise) is considered as the chief noise, without concerning other internal noises, such as Johnson noise, thermal fluctuation, and $1/f$ noise. In addition, for characterizing how highly the photogenerated carriers excited by per incident photons in photodetector, EQE is 8.6×10^4 % as calculated by Eq. (6). Besides, the linearity in a photodetector *versus* light intensity is seriously vital for quantitative study, figure 4(c) gives the relationship between the I_{photo} and light intensity (in units of μW/cm^2), according to a power law of $I_{photo}\propto P^\theta$, the value of θ is calculated to

be 0.94, which is many close to 1, which suggests less carrier scattering and electron–hole recombination in this photodetector. The linearity of a photodetector is a serious issue for actual quantized application of photosensing device. The high value of indicates a linear relationship between photogenerated electron–hole pairs and the incident light intensity.[35] Moreover, the R, D^*, and EQE display decreasing trend as the incident DUV light intensity increases from 300 μW/cm^2 to 800 μW/cm^2 as shown in Fig. 4(d), because of that high-intensity light illumination leads to the carrier scattering and enhanced recombination (between photogenerated electrons and holes).

Figure 5(a) shows the time-dependent current (I–t) performance of the ε-Ga_2O_3 thin film photodetector under 254-nm DUV light illumination with intensities of 300 μW/cm^2, 400 μW/cm^2, 500 μW/cm^2, 600 μW/cm^2, and 800 μW/cm^2 at 5 V, suggesting an ability to follow the fast-changing light signal. Figure 5(b) shows the response time by fitting of the I–t curves at 5 V under illumination with light intensity of 300 μW/cm^2, based on an exponential relaxation equation[36]

$$I = I_0 + A\,\mathrm{e}^{-t/\tau}, \tag{7}$$

where I_0 is stable I_{photo}, A is constant, t is the time, and τ is the relaxation time constant. The rise time and decay time are shown as τ_r and τ_d, respectively. For this photodetector in this work, the τ_r and τ_d are 0.38 s and 0.13 s, respectively. In Table 1, a comparison of ε-Ga_2O_3-based photodetectors is shown. Besides, the ε-Ga_2O_3 solar-blind photodetector shows good photo response performance, and shows high solar-blind rejection ratio of 1.2×10^6 and high photocurrent gain of more than 800.

Table 1. A comparison of ε-Ga_2O_3-based photodetectors.

Layout	I_{dark} (A)	PDCR	R (A/W)	D^* (Jones)	EQE (%)	Refs.
MSM	–	3.9×10^7	262.1	4.73×10^{14}	–	[37]
MSM	2.72×10^{-12}	$\sim10^3$	2.52×10^{-3}	2.49×10^{11}	–	[38]
Flexible MSM	–	1.66×10^7	703	4.08×10^{14}	3.9×10^5	[39]
Si-gated phototransistor	–	$\sim10^6$	9362.4	8.82×10^{15}	–	[40]
MSM	2.35×10^{-11}	–	230	1.2×10^{15}	–	[16]
MSM	9.85×10^{-11}	1.68×10^2	0.0772	2.85×10^{12}	37.8	[21]
MSM	1.87×10^{-11}	1.82×10^4	0.52	1.67×10^{13}	–	[20]
MSM	1.52×10^{-12}	8.78×10^6	175.69	2.46×10^{15}	8.6×10^4	this work

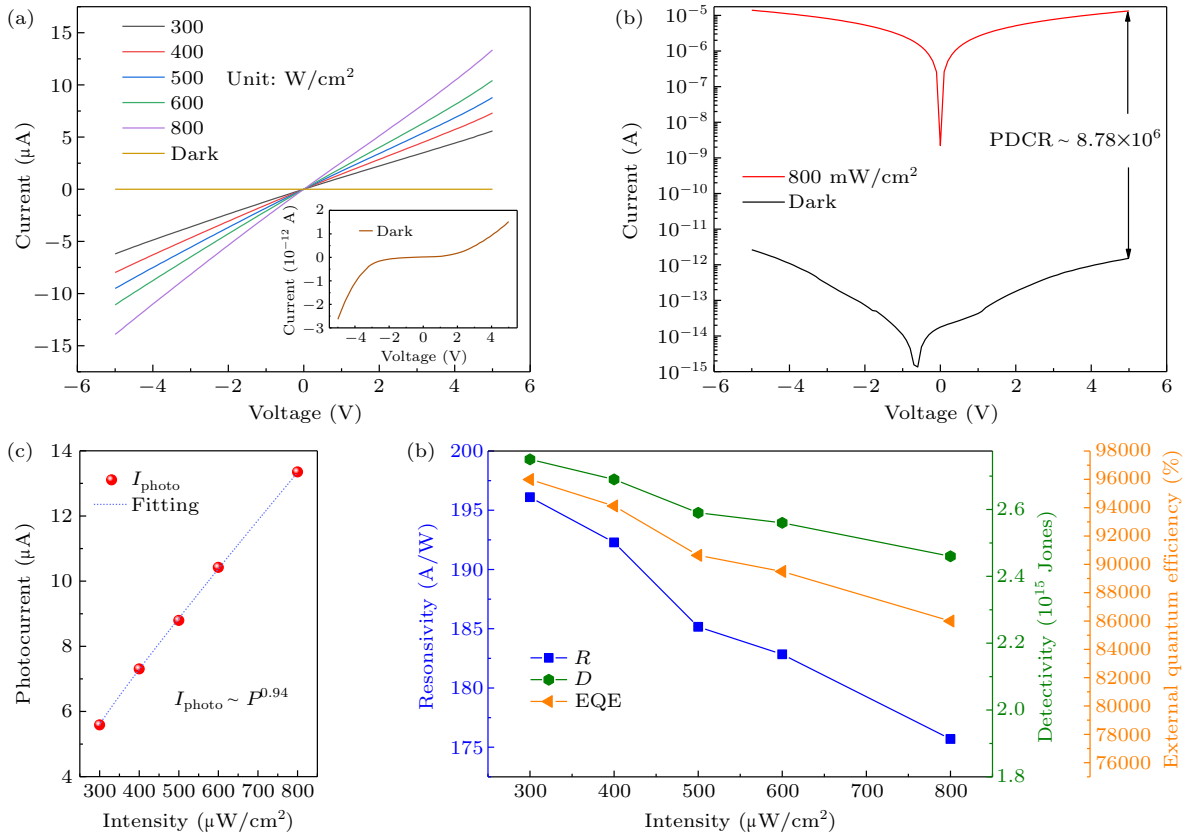


Fig. 4. (a) The I–V curves under illuminations with various light intensities from −5 V to 5 V, (b) the semi-log I–V curve under illumination with light intensity of 800 μW/cm^2 of the ε-Ga_2O_3 thin film photodetector. The light intensity-dependent (c) photocurrent and (d) responsivity, detectivity, and external quantum efficiency.

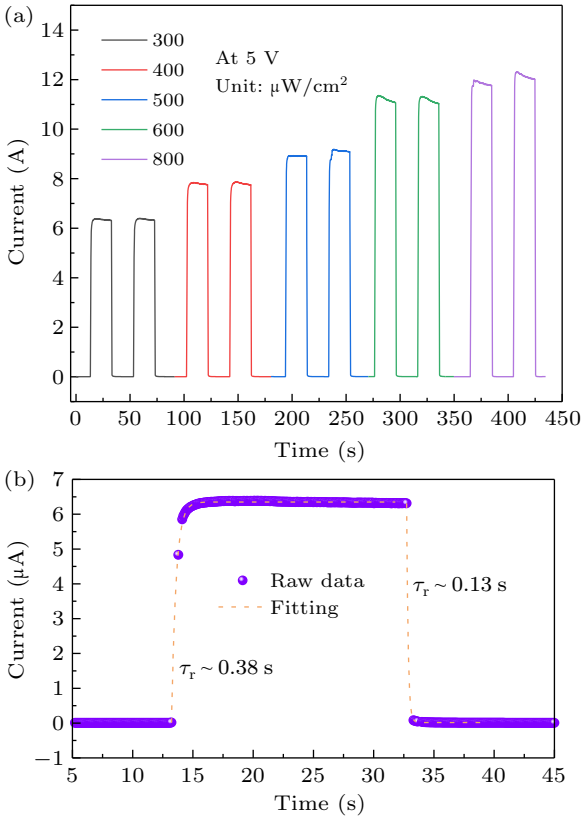


Fig. 5. (a) Transient photoresponse of the ε-Ga_2O_3 photodetector under illumination with various light intensities, (b) its time response characteristic under 254-nm light illumination with an intensity of 300 μW/cm^2 at 5 V.

In Fig. 6(a), the relationship between DUV light intensity and photocurrent gain (G) is given at room temperature. Considering that all incident photons are absorbed (*i.e.*, the internal quantum efficiency is ~ 1), the photocurrent G is calculated to be ~ 859 at 5 V when the DUV light intensity is 800 μW/cm^2, based on a relationship[41,42]

$$G = \frac{(I_{\text{photo}} - I_{\text{dark}})/q}{PS/hv}, \tag{8}$$

where hv is the photon energy of the incident photon. The photocurrent G decreases as the light intensity increases as shown in Fig. 5(b). This phenomenon is owing to the recombination of photogenerated carriers caused by the large photon flux for larger light intensity. The obtained large photocurrent G here is quite high due to the recycling gain mechanism, the carriers could transport many times in the channel layer in the photodetector until the photogenerated electrons and holes recombine. In this respect, the photodetector shows that the carriers are highly collected by the electrodes relative to the incident photons by carrier multiplication process and minority carrier trapping effect.[43] That is, for n-type Ga_2O_3 semiconductor, the minority carriers (holes) may well be trapped in the recombined center of Ga_2O_3, so as to that it is in trouble for recombination with the majority carrier (electrons), as displayed in Fig. 6(b),[44] thus, the remaining electrons will transport more than one time between the two electrodes in photodetector, yielding multiple passes through the active layer, and high photocurrent G is shown. Generally, under consideration, the trapped carriers are owing to the underlying defects at the Schottky Ni/Ga_2O_3 interface, the thickness of the depletion layer becomes smaller, lots of the additional carriers may tunnel in the Ga_2O_3 semiconductor, so the photocurrent G is far larger than unity. The further improvement and modulation of the metal–semiconductor–metal Schottky photodetector response characterizations could provide an efficient method for developing high-performance DUV photodetectors. Especially for the metastable Ga_2O_3, such as the ε-Ga_2O_3 in this work, the study of the photocurrent G and corresponding mechanism are seriously necessary towards the new-generation DUV photodetector.

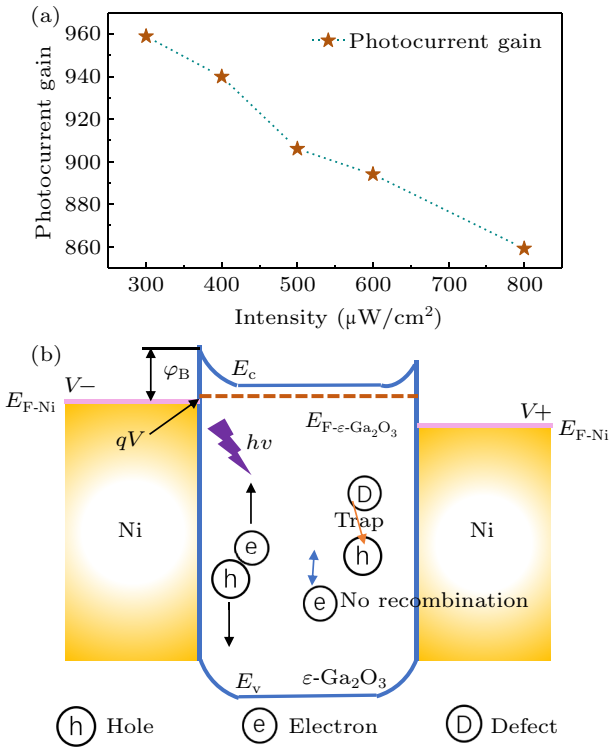


Fig. 6. (a) Curve of photocurrent gain dependent on the incident light intensity, (b) energy-band diagram of the photodetector under illumination at a voltage.

4. Conclusion

In this paper, the ε-Ga_2O_3 thin film was grown by using MOCVD, and a DUV PD is constructed. In addition to the high quality of film crystal. The photodetector displayed decent photoresponse performance, including R of 175.69 A/W, D^* of 2.46×10^{15} Jones, EQE of 8.6×10^4% and highly photocurrent-intensity linearity. The large photocurrent G of 849 is owing to the recycling gain mechanism; and it decreases as the incident light intensity increases because of the recombination of photogenerated carriers by the large photon flux when large intensity light is irradiated on the surface of the photodetector.

Acknowledgment

Project supported by the National Natural Science Foundation of China (Ganrt No. 62004047).

References

[1] Tsao J Y, Chowdhury S, Hollis M A, Jena D, Johnson N M, Jones K A, Kaplar R J, Rajan S, Van de Walle C G, Bellotti E, Chua C L, Collazo R, Coltrin M E, Cooper J A, Evans K R, Graham S, Grotjohn T A, Heller E R, Higashiwaki M, Islam M S, Juodawlkis P W, Khan M A, Koehler A D, Leach J H, Mishra U K, Nemanich R J, Pilawa-Podgurski R C N, Shealy J B, Sitar Z, Tadjer M J, Witulski A F, Wraback M and Simmons J A 2017 *Adv. Electron. Mater.* **4** 1600501

[2] Hudgins J L, Simin G S, Santi E and Khan M A 2003 *IEEE Trans. Power Electron.* **18** 907

[3] Chen X, Ren F, Gu S and Ye J 2019 *Photon. Res.* **7** 381

[4] Liu Z, Li P, Zhi Y, Wang X, Chu X and Tang W 2019 *Chin. Phys. B* **28** 017105

[5] Liu Z, Zhi Y, Zhang M, Yang L, Li S, Yan Z, Zhang S, Guo D, Li P, Guo Y and Tang W 2022 *Chin. Phys. B* **31** 088503

[6] Tippins H H 1965 *Phys. Rev.* **140** A316

[7] Qian L, Li W, Gu Z, Tian J, Huang X, Lai P T and Zhang W 2022 *Adv. Opt. Mater.* **10** 2102055

[8] Zhi Y S, Liu Z, Zhang S H, Li S, Yan Z Y, Li P G and Tang W H 2021 *IEEE Trans. Electron Dev.* **68** 3435

[9] Zhou X, Zhang X, He T, Ma Y, Zhang L, Chen T, Wei X, Tang W, Fan Y, Cai Y, Zhang B and Zhang X 2021 *J. Phys. D: Appl. Phys.* **54** 445103

[10] Liu Z, Zhang M, Yang L, Li S, Zhang S, Li K, Li P, Guo Y and Tang W 2022 *Semicond. Sci. Technol.* **37** 015001

[11] Li Z, Feng Z, Xu Y, Feng Q, Zhu W, Chen D, Zhou H, Zhang J, Zhang C and Hao Y 2022 *IEEE Trans. Electron Dev.* **69** 1143

[12] Liu Z, Wang X, Liu Y, Guo D, Li S, Yan Z, Tan C K, Li W, Li P and Tang W 2019 *J. Mater. Chem. C* **7** 13920

[13] Liu Z, Li S, Yan Z, Liu Y, Zhi Y, Wang X, Wu Z, Li P and Tang W 2020 *J. Mater. Chem. C* **8** 5071

[14] Jiang W, Liu Z, Li S, Yan Z, Lu C, Li P, Guo Y and Tang W 2021 *IEEE Sensors J.* **21** 18663

[15] Qiao B, Zhang Z, Xie X, Li B, Chen X, Zhao H, Liu K, Liu L and Shen D 2021 *J. Mater. Chem. C* **9** 4039

[16] Qin Y, Li L, Zhao X, Tompa G S, Dong H, Jian G, He Q, Tan P, Hou X, Zhang Z, Yu S, Sun H, Xu G, Miao X, Xue K, Long S and Liu M 2020 *ACS Photon.* **7** 812

[17] Zhou H, Cong L, Ma J, Li B, Chen M, Xu H and Liu Y 2019 *J. Mater. Chem. C* **7** 13149

[18] Alfaraj N, Li K H, Alawein M, Kang C H, Braic L, Zoita N C, Kiss A E, Ng T K and Ooi B S 2021 *Adv. Mater. Technol.* **6** 2100142

[19] Zheng W, Lin R, Zhang D, Jia L, Ji X and Huang F 2018 *Adv. Opt. Mater.* **6** 1800697

[20] Liu Z, Huang Y, Zhang C, Wang J, Li H, Wu Z, Li P and Tang W 2020 *J. Phys. D: Appl. Phys.* **53** 295109

[21] Liu Z, Huang Y, Li H, Zhang C, Jiang W, Guo D, Wu Z, Li P and Tang W 2020 *Vacuum* **177** 109425

[22] Li S, Yue J Y, Lu C, Yan Z Y, Liu Z, Li P G, Guo D Y, Wu Z P, Guo Y F and Tang W H 2022 *Sci. China Tech. Sci.* **65** 704

[23] Wang Z, Gong H, Meng C, Yu C, Sun X, Zhang C, Ji X, Ren F, Gu S, Zheng Y, Zhang R and Ye J 2022 *IEEE Trans. Electron Dev.* **69** 981

[24] Katz O, Bahir G and Salzman J 2004 *Appl. Phys. Lett.* **84** 4092

[25] Morgan B J and Madden P A 2011 *Phys. Rev. Lett.* **107** 206102

[26] Mezzadri F, Calestani G, Boschi F, Delmonte D, Bosi M and Fornari F 2016 *Inorg. Chem.* **55** 12079

[27] Chen Z, Li Z, Zhuo Y, Chen W, Ma X, Pei Y and Wang G 2018 *Appl. Phys. Express* **11** 101101

[28] Liu Z, Zhi Y, Li S, Liu Y, Tang X, Yan Z, Li P, Li X, Guo D, Wu Z and Tang W 2020 *J. Phys. D: Appl. Phys.* **53** 085105

[29] Thomson G W 1946 *Chem. Rev.* **38** 1

[30] Yang J, Sparks Z, Ren F, Pearton S J and Tadjer M J 2018 *J. Vac. Sci. Technol. B* **36** 061201

[31] Schultz T, Vogt S, Schlupp P, von Wenckstern H, Koch N and Grundmann M 2018 *Phys. Rev. Appl.* **9** 064001

[32] Ma G, Jiang W, Sun W, Yan Z, Sun B, Li S, Zhang M, Wang X, Gao A, Dai J, Liu Z, Li P and Tang W 2021 *Phys. Scr.* **96** 125823

[33] Zhang S, Liu Z, Liu Y, Zhi Y, Li P, Wu Z and Tang W 2021 *Micromachines* **12** 259

[34] Liu Z, Du L, Zhang S, Li L, Xi Z, Tang J, Fang J, Zhang M, Yang L, Li S, Li P, Guo Y and Tang W 2022 *IEEE Trans. Electron Dev.* **69** 5595

[35] Taylor G W and Simmons J G 1972 *J. Non-Cryst. Solids* **8–10** 940

[36] Liu N, Fang G, Zeng W, Zhou H, Cheng F, Zheng Q, Yuan L, Zou X and Zhao X 2010 *ACS Appl. Mater. Interfaces* **2** 1973

[37] Zhou S, Zhang H, Peng X, Liu H, Li H, Xiong Y, Li W, Yang P A, Ye L and Kong C 2022 *Adv. Photon. Res.* **3** 2200192

[38] Yang Y, Zhu H, Wang L, Jiang Y, Wang T, Liu C, Li B, Tang W, Wu Z, Yang Z and Li D 2022 *Materials & Design* **221** 110944

[39] Lu Y, Krishna S, Tang X, Babatain W, Hassine M B, Liao C H, Xiao N, Liu Z and Li X 2022 *ACS Appl. Mater. Interfaces* **14** 34844

[40] Zhou X, Zhang X, He T, Ma Y, Zhang L, Chen T, Wei X, Tang W, Fan Y, Cai Y, Zhang B and Zhang X 2021 *J. Phys. D: Appl. Phys.* **54** 445103

[41] Garrido J A, Monroy E, Izpura I and Muñoz E 1998 *Semicond. Sci. Technol.* **13** 563

[42] Soci C, Zhang A, Bao X Y, Kim H, Lo Y and Wang D 2010 *J. Nanosci. Nanotechnol.* **10** 1430

[43] Hu G C, Shan C X, Zhang N, Jiang M M, Wang S P and Shen D Z 2015 *Opt. Express* **23** 13554

[44] Li C, Bando Y, Liao M, Koide Y and Golberg D 2010 *Appl. Phys. Lett.* **97** 161102